CHAPTER: 4 Binuclear complexes with σ-bonded bridged

4.1 Introduction:

The study of binuclear copper (II) complexes is a topic of considerable current interest because of their use as models for a number of important biological systems containing coupled binuclear active sites [1-5]. The focus of much of this work has been on magnetic exchange interaction [6, 7] between the two copper (II) ions which may be diagnostic for the nature and geometry of the ligand – bridged binuclear centre. These efforts have resulted in a better fundamental understanding of spin exchange through long σ – bonded bridges and of molecular materials exhibiting new but considerable magnetic properties [8, 9].

The extent of spin exchange between two copper (II) centers depends on the energy of the interacting orbitals and on the variation in geometrical parameters such as metal – ligand bond length, M-L-M bridging angle, dihedral angle between the metal coordination plane and the degree of planarity of the bridging unit [10-14]. In most cases this type of exchange through multi atomic bridges has been shown to take place through the orbitals of the bridging ligand. However, recently it has been suggested that the σ – orbitals [15, 16] can participate in the super exchange over a long distance in multiatomic bridges and lead to a spin exchange [17-19], yet such interactions are very weak. Variation in the bridging ligand can directly affect the nature of the bridging molecular orbital participating in the exchange where as change in the non bridging part of the ligand can affect the energy of the metal orbital and the coordination geometry .

In order to study magnetic exchange between paramagnetic metal centers through saturated organic groups, new binuclear $[Cu_2L_2](SO_4)_2$ and ternary $[Cu_2L(AA)](X)_4$ complexes have been synthesized . The ligands are L^1 = N,N'-bis(2-pyridylcarbonyl)-1,4-diaminobutane (picbu) and L^2 = N,N'-bis(2-pyridylcarbonyl)-1,6-diaminohexane (pichx) and AA = 2,2'-bipyridyl or 1,10-phenanthroline or 2-hydroxybenzoic acid or 5-bromo-2-hydroxybenzoic acid . The complexes have been characterized based on elemental analysis and spectral properties. The FAB mass spectra of complexes are consistent with the binuclear formulation. Semi empirical

quantum mechanical calculation has been used to work out the geometrical parameters in various complexes and the suitability of the bridging ligand orbitals to propagate any spin exchange, these have been correlated with the magnetic property.

4.2 Experimental

4.2.1 Chemicals:

Ethyl-2-pyridinecarboxylate, 1,4-diaminobutane, 1,6-diaminohexane 2-hydroxybenzoic acid and sodium sulphate dihydrate were obtained from Merck. All of these were of A. R. grade and were used as received. All other chemicals were used, as described in previous chapters.

5-bromo-2-hydroxybenzoic acid was prepared by low temperature (5 °C, ice – salt bath) bromination of 2-hydroxybenzoic acid. Yield: 60.00%, mp 164-166 °C (Lit.: 164–166 °C) [20].

4.2.2 Physical measurements:

The elemental analysis, thermal analysis and conductivity measurements were carried out as described in chapter 3.

UV-VIS, IR, ESR and FAB-Mass spectral analysis was done using the instruments described in chapter 3.

^{1}H NMR of the ligand was recorded on the same instrument as in chapter 2.

The details of magnetic measurements are as described in detail in the earlier chapters.

4.2.3 Synthesis of binucleating ligands:

4.2.3.1 N,N'-bis(2-pyridylcarbonyl)-1,4-diaminobutane (picbu):

A solution of ethyl-2-pyridinecarboxylate (3.779 g, 3.40 ml, 25 mmol) was placed in a flask equipped with water condenser and a magnetic stirrer. To this was

added a solution of 1,4-diaminobutane (1.102 g, 1.25 ml, 12.5 mmol) . The mixture was allowed to reflux for nine hours while monitoring the progress of reaction by TLC. A pale yellow solid compound separated out on cooling. The solid product obtained was crystallized from 50:50 $CHCl_3$ and petroleum ether. Finally, the compound was washed with 20 ml (in five portions) distilled water and 10 ml diethylether and was dried in air.

Yield : 2.528 g, (40%), mp : 107 -110 °C.

Elemental analysis : (obsd.) %C 64.66, %H 5.97, %N 18.76.

(calc. for the formula, $C_{16}H_{18}N_4O_2$) %C 64.43, %H 6.04, %N 18.79.

Important IR frequencies (KBr disc, $\bar{\nu}$ in cm^{-1}): 3358, 3066, 2945, 2856, 1657, 1593.

4.2.3.2 N,N'-bis(2-pyridylcarbonyl)-1,6-diaminohexane (pichx) :

Solution of ethyl-2-pyridinecarboxylate (3.779 g, 3.40 ml, 25 mmol) was placed in a flask equipped with water condenser and a magnetic stirrer. To this was added solution of 1,6-diaminohexane (1.453 g, 1.70 ml, 12.5 mmol) . The mixture was refluxed for nine hours, on cooling pale yellow compound separated. The solid obtained was crystallized from 50:50 $CHCl_3$ and petroleum ether. Finally the compound was washed with 20 ml (in five portions) distilled water and 10 ml diethylether and dried in air.

Yield : 3.172 (39%), mp : 97 -100 °C.

Elemental analysis : (obsd.) %C 66.26, %H 6.47, %N 17.09.

(calc. for the formula, $C_{18}H_{22}N_4O_2$) %C 66.26, %H 6.74, %N 17.18.

Important IR frequencies (KBr disc, $\bar{\nu}$ in cm^{-1}): 3371, 3068, 2924, 2853, 1657, 1593.

Chemical shift values in ^1H NMR recorded in $CDCl_3$ solution: (δ)1.494 (t, 4H (CH_2)); 1.696 (t, 4H (CH_2)); 3.492 (q, 4H (CH_2)); 7.444 (t, 2H (NH)); 7.841 (t, 2H (PyH); 8.086 (s, 2H (PyH); 8.215 (d, 2H (PyH); 8.552 (d, 2H (PyH) (**Fig. 4.1.1 to Fig. 4.1.3).**

4.2.4 Preparation of the Complexes:

4.2.4.1 Preparation of binuclear $[Cu_2(picbu)_2](SO_4)_2$ and $[Cu_2(pichx)_2](SO_4)_2$ complex, (4-I, 4-II):

Copper (II) acetate monohydrate (0.295 g, 1.25 mmol) was dissolved in 20 ml CH_3OH and to this, a solution of ligand picbu (0.373 g, 1.25 mmol) in 20 ml of CH_3OH was added dropwise with constant stirring and heating. The solution was allowed to reflux for two hours. Excess of CH_3OH (25 ml) was distilled out, the reaction mixture was cooled and ~ 25 ml distilled water was added. A solution of anhydrous sodium sulphate (0.178 g, 1.25 mmol) in 10 ml distilled water was added and the solution was digested for 30 minutes on water bath. The light green coloured solid obtained was filtered and washed with small portions of 50 ml water followed by 30 ml CH_3OH. The product (**4-I**) was dried in air.

$[Cu_2(pichx)_2](SO_4)_2$, (**4-II**) was prepared by following a similar procedure and using 0.408g (1.25 mmol) of pichx in place of picbu (**Scheme 4.1**).

4.2.4.2 Preparation of binuclear $[Cu_2(AA)_2picbu](X)_4$ type complexes, (4-III to 4-VI):

Copper (II) acetate monohydrate (0.333 g, 1.66 mmol) in 20 ml CH_3OH was taken in three neck flat bottom flask. To this was added 1,10-phenanthroline (0.330 g, 1.67 mmol) in 15 ml CH_3OH and picbu (.248 g, 0.83 mmol) in 15 ml CH_3OH simultaneously dropwise over 1 hour. The reaction mixture was allowed to reflux for two hours. The excess of CH_3OH was distilled out from reaction mixture, 20 ml distilled water followed by sodium perchlorate monohydrate (0.468 g, 3.33 mmol) in 10 ml distilled water were added. The solution was allowed to digest for 30 minutes on water bath. Light blue coloured solid separated on cooling was filtered, washed thoroughly with 50 ml distilled water followed by 25 ml ethanol and dried in air (**4-III**).

4.2.4.3 Preparation of binuclear $[Cu_2(AA)_2picbu]$ type complexes, (4-VII to 4-X):

A solution of copper (II) acetate monohydrate (0.333 g, 1.66 mmol) in 20 ml methanol was taken in a three neck flask. Solution of 0.230 g (1.67 mmol) of 2-

hydroxybenzoic acid and 0.248 g (0.83 mmol) of picbu, each in 15 ml methanol, were added dropwise with constant stirring over 1 hour to the hot refluxing solution of copper (II) acetate. The solution was allowed to reflux for further 2 hours where upon a micro crystalline solid separated out. It was filtered, washed thoroughly with ~ 30 ml methanol and dried in air (**4-VII**).

Complexes, **4-VIII** was prepared by following similar procedure as above and using picbu by 0.272 g (0.83 mmol) of pichx in place of picbu. Complexes, **4-IX** and **4-X** were synthesized by similar procedure and using 5-bromo-2-hydroxybenzoic acid and either picbu or pichx, respectively, (**Scheme 4.2**).

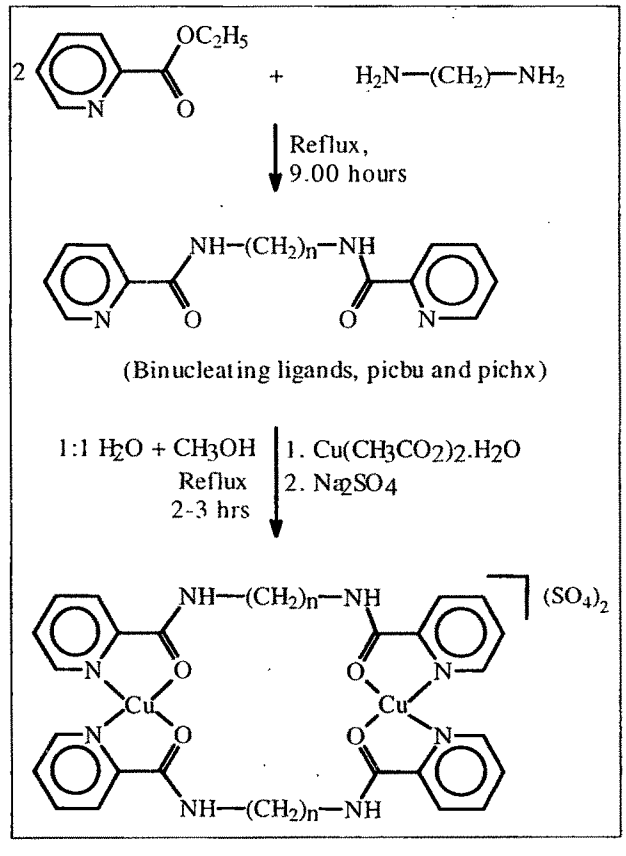

4-I : n = 4.
4-II : n = 6.

Scheme 4.1 Synthesis of binuclear complexes, **4-I** and **4-II**.

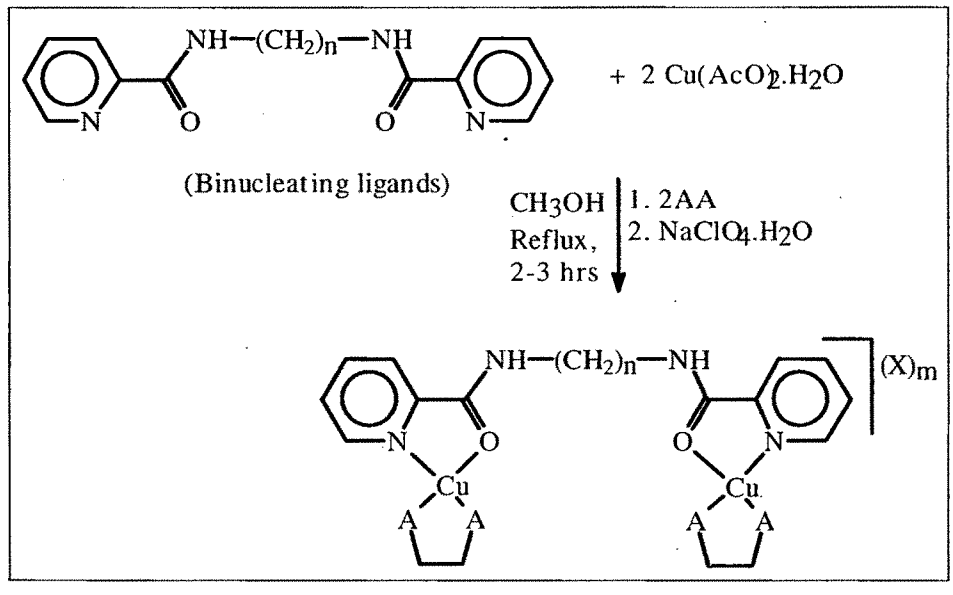

4-III : AA = phen, n = 4, X = ClO_4^-, m = 4.

4-IV : AA = phen, n = 6, X = ($3ClO_4^-$, $CH_3CO_2^-$), m = 4.

4-V : AA = bipy, n = 4, X = ClO_4^-, m = 4.

4-VI : AA = bipy, n = 6, X = ($3ClO_4^-$, $CH_3CO_2^-$), m = 4.

4-VII : AA = 2-hydroxybenzoic acid, n = 4, X = 0.

4-VIII : AA = 2-hydroxybenzoic acid, n = 6, X = 0.

4-IX : AA = 5-bromo-2-hydroxybenzoic acid, n = 4, X = 0.

4-X : AA = 5-bromo-2-hydroxybenzoic acid, n = 6, X = 0.

Scheme 4.2 Synthesis of binuclear complexes, **4-III** to **4-X**.

4.3 Results and discussion:

The purified ligands have elemental analysis consistent with the empirical formula. The proton NMR of the ligand (**Fig. 4.1.1 to Fig. 4.1.3**) have all feature expected for the proposed structures. The assignment of lines in ^1H NMR to various types of protons in the molecule is shown in **Fig. 4.1 and Fig. 4.1.1.**

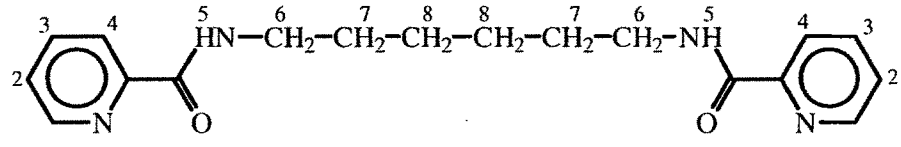

Fig 4.1 Types of protons in binucleating ligand, pichx.

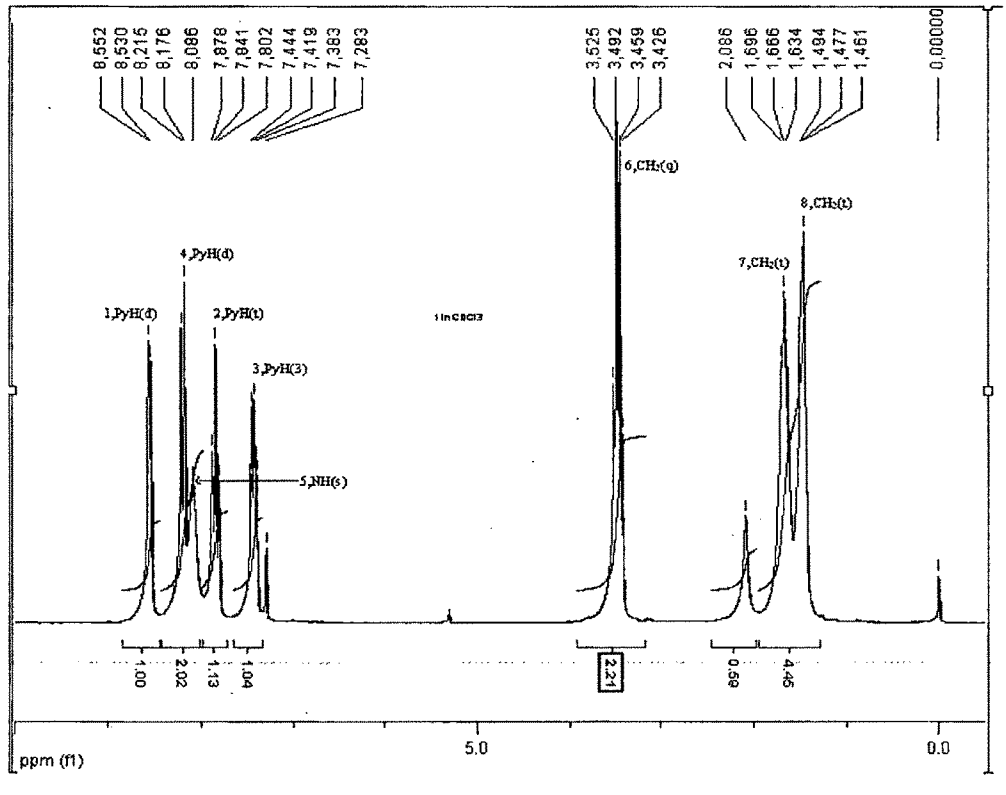

Fig. 4.1.1 ^1H NMR spectrum of the ligand, pichx in $CDCl_3$.

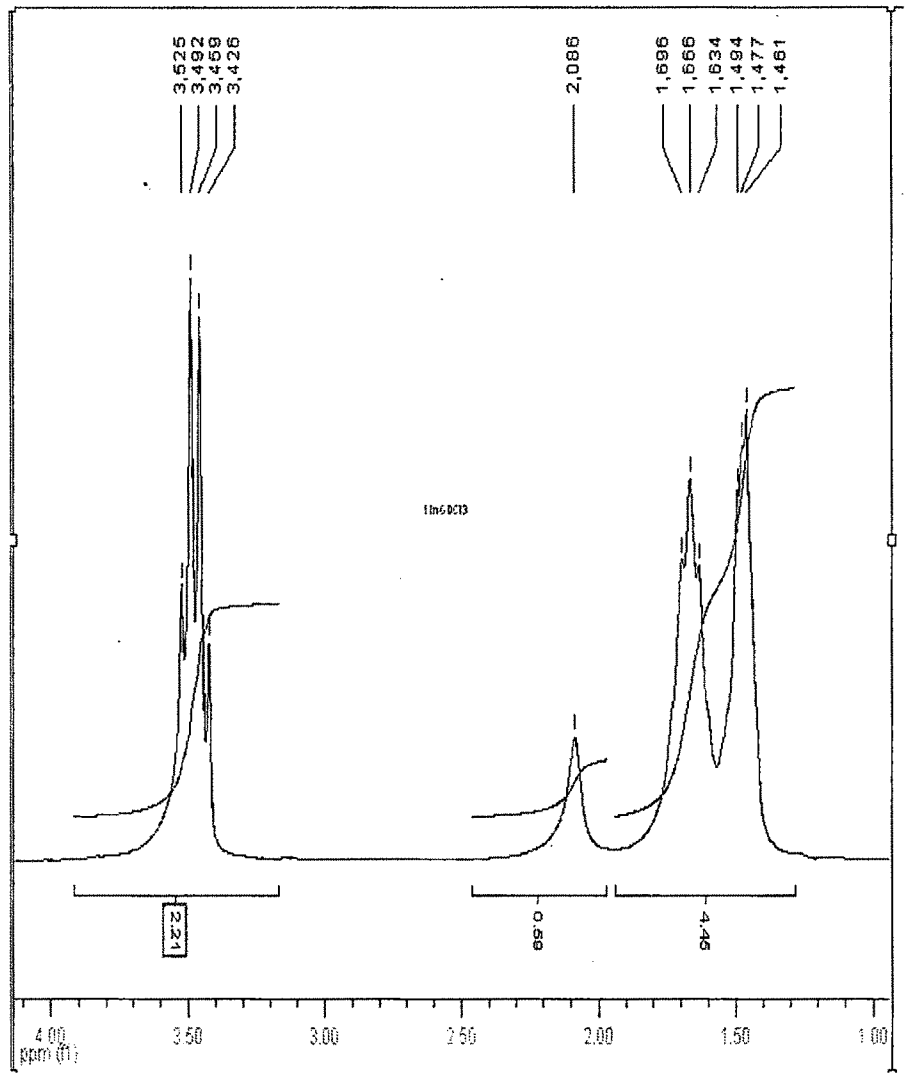

Fig. 4.1.2 ^{1}H NMR spectrum of the ligand, pichx in $CDCl_3$ (expanded).

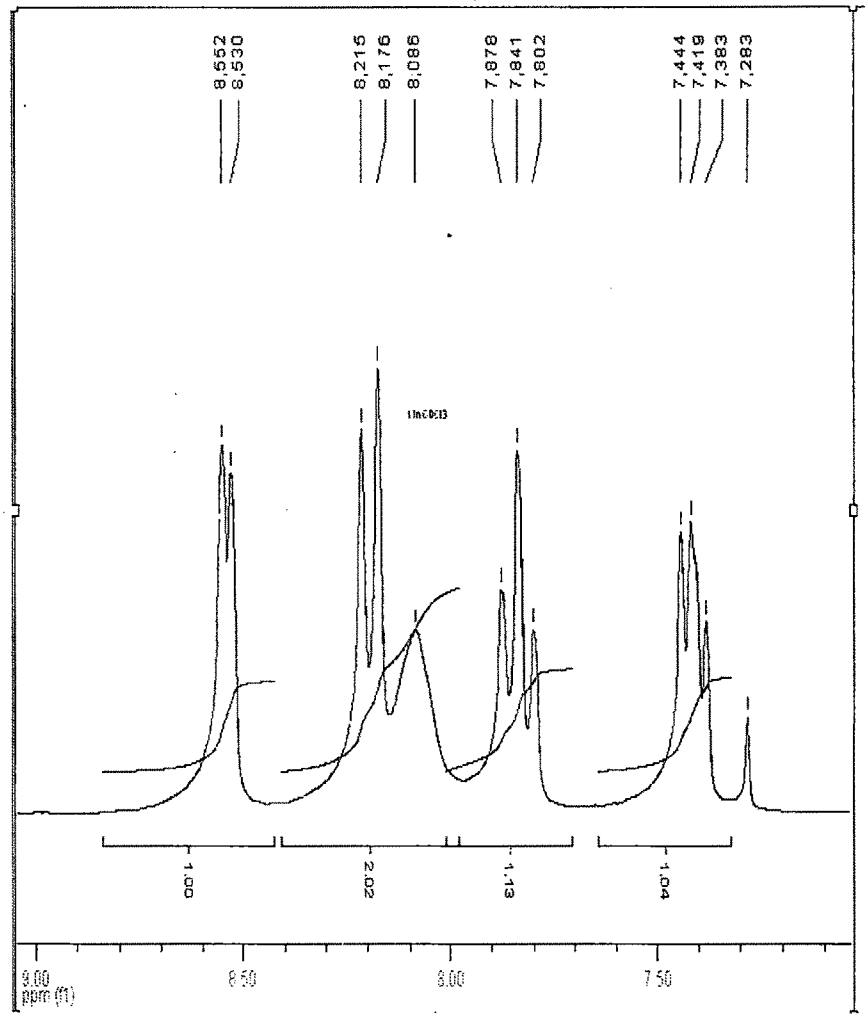

Fig. 4.1.3 ^{1}H NMR spectrum of the ligand, pichx in $CDCl_3$ (expanded)

The binucleating ligand, bis(picolinamide) is ambidentate and can coordinate with the metal ion either (1) through the amide nitrogen or (2) the amide oxygen. In both cases, it will form five membered chelate rings with the metal ion (**Fig. 4.2.1** & **fig 4.2.2**).

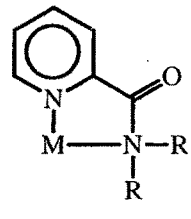

Fig. 4.2.1

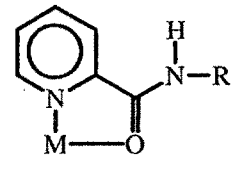

Fig. 4.2.2

In order to verify the preference for coordination, the ligand geometries were optimized by semi-empirical Quantum Mechanical (PM3) calculations and the energy, electrostatic potentials and electron densities were calculated. The map of electrostatic potential over electron density shows maximum electron density (**Fig. 4.3** and **Fig. 4.4)** over pyridine nitrogen and amide oxygen directed towards each other in a way to facilitate the coordination of a metal ion at this site and confirms the coordination through amide nitrogen (**Fig. 4.2.2).**

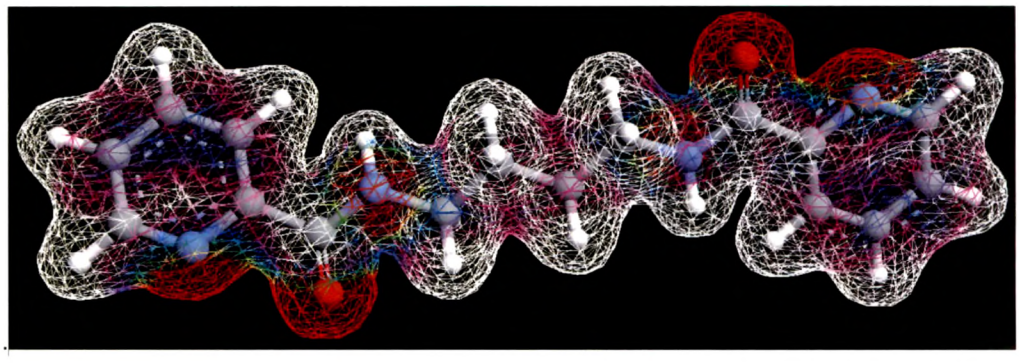

Fig. 4.3 Plot of electrostatic potential over elecronegativity of ligand, picbu.

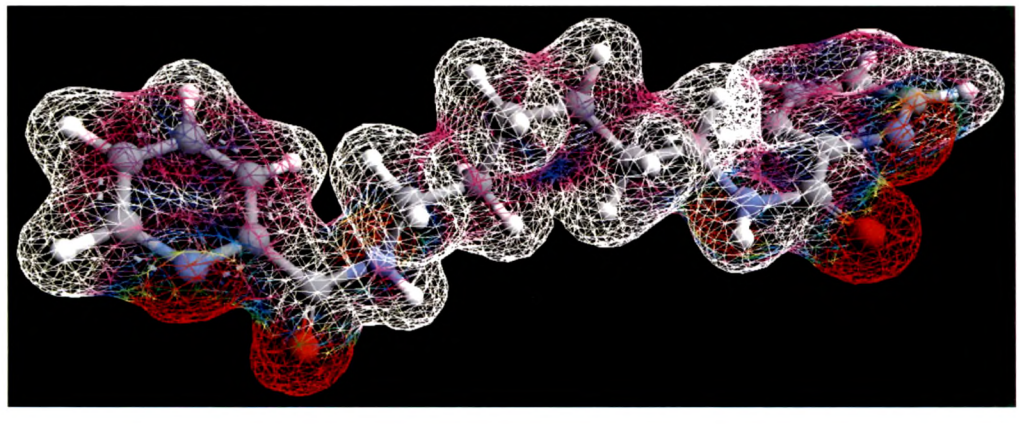

Fig. 4.4 Plot of electrostatic potential over elecronegativity of ligand, pichx.
(Red regions indicate region richer in electronegativity)

The elemental analysis of the binuclear complexes correspond to expected formula given in **Table 4.1**. The generalized molecular formulae structures of the symmetrical binary and ternary binuclear complexes can be represented as shown in **scheme 4.1 and 4.2** respectively. The ionic complexes of ligand, picbu, crystallized with four perchlorate anions while those formed by ligand, pichx crystallized with one acetate and three perchlorate anions.

The molar conductivity measurements were carried out using 1.0 mmol solutions of complexes in DMF to confirm the number of anions present in the complexes. Complexes **4-III, 4-IV** and **4-V** have molar conductivity values between 280 – 300 $\Omega^{-1}cm^2mol^{-1}$. The values correspond to 1:4 electrolytes, indicating the presence of four anions. Complex **4-VI** has molar conductivity value of 220 $\Omega^{-1}cm^2mol^{-1}$ corresponding to 1:3 electrolyte. This indicates that only three anions i.e. perchlorate ions are ionisiable and must be outside the coordination sphere while one acetate ion present in the complex must be coordinated with the metal ions. Complexes **4-I** and **4-II,** though ionic, are insoluble in suitable solvents and hence conductivity measurements could not be performed.

The TGA in the temperature range 50 – 600 °C shows that there is loss of water molecules between 140 – 210 °C. In complex **4-I,** the loss in weight corresponds to eight water molecules and in complex **4-II** loss in weight corresponds to four water molecules (**Table 4.1**). The loss of water molecules takes place at such high temperature, indicating that the water molecules are either coordinated to the metal ion or they are held by hydrogen bonding. The sulphate ions are known to form strong H – bonds with water molecules and hence the sulphate salts are often associated with H – bonded water in their crystals. This must be the reason for high water contents in these complexes.

Table 4.1: Reflux time, yields, elemental analysis, thermal analysis and molar conductivity of the binuclear complexes of bis(picolinamide)ligands.

Comp No.	Complexes	Reflux Time (hours)	Yield (%)	Elemental analysis Obsd. (Calc) in %			Temp. Range (°C)	% wt loss of H_2O	Molar conductivity ($\Omega^{-1}cm^2mol^{-1}$)
				C	H	N			
4-I	$[Cu_2(picbu)_2](SO_4)_2.8H_2O$	2	56	36.87	4.80	10.85	140-210	14.82	Not Soluble
	$C_{32}H_{42}N_8O_{20}S_2Cu_2$			(36.26)	(4.91)	(10.57)		(13.60)	
4-II	$[Cu_2(pichx)_2](SO_4)_2.4H_2O$	2	52	40.55	4.55	10.63	170-210	8.19	Not Soluble
	$C_{36}H_{52}N_8O_{20}S_2Cu_2$			(41.41)	(4.98)	(10.73)		(6.90)	
4-III	$[Cu_2(phen)_2(picbu)](ClO_4)_4$	4	57	41.42	3.04	9.37	-	-	290
	$C_{40}H_{34}N_8O_{18}Cl_4Cu_2$			(40.57)	(2.87)	(9.47)			
4-IV	$[Cu_2(phen)_2(pichx)](ClO_4)_3(Ac)_1$	4	66	45.16	3.42	9.87	-	-	280
	$C_{44}H_{41}N_8O_{16}Cl_3Cu_2$			(45.10)	(3.50)	(9.56)			
4-V	$[Cu_2(bipy)_2(picbu)](ClO_4)_4$	3	52	39.22	3.47	10.65	-	-	300
	$C_{36}H_{34}N_8O_{18}Cl_4Cu_2$			(38.06)	(2.99)	(9.86)			
4-VI	$[Cu_2(bipy)_2(pichx)(Ac)](ClO_4)_3$	4	31	44.50	3.89	11.46	-	-	220
	$C_{40}H_{41}N_8O_{16}Cl_3Cu_2$			(42.77)	(3.65)	(9.98)			

Continued.....

Comp No.	Complexes	Reflux Time (hours)	Yield (%)	Elemental analysis Obsd. (Calc) in % C	H	N	Temp. Range (°C)	% wt loss of H_2O	Molar conductivity ($\Omega^{-1}cm^2mol^{-1}$)
4-VII	$[Cu_2(salacid)_2(picbu)]$	2	83	51.57	3.70	8.22	-	-	-
	$C_{30}H_{26}N_4O_8Cu_2$			(51.64)	(3.73)	(8.03)			
4-VIII	$[Cu_2(salacid)_2(pichx)].2H_2O$	2	50	49.33	4.05	6.58	135-200	5.10	-
	$C_{32}H_{34}N_4O_{10}Cu_2$			(50.45)	(4.46)	(7.35)		(4.73)	
4-IX	$[Cu_2(Brsalac)_2(picbu)]$	3	85	41.47	2.97	6.42	-	-	-
	$C_{30}H_{24}N_4O_8Br_2Cu_2$			(42.10)	(2.80)	(6.54)			
4-X	$[Cu_2(Brsalac)_2(pichx)]$	3	91	45.02	3.71	6.85	-	-	-
	$C_{32}H_{32}N_4O_{10}Br_2Cu_2$			(43.48)	(3.17)	(6.34)			

The values given in parentheses are theoretical values calculated from the molecular formulae.

4.3.1 Electronic Spectra:

The electronic spectra of the binuclear complexes in methanolic solutions show several bands in the range of 200 – 850 nm. Intense bands observed below 350 nm are due to interligand transitions. The weak and broad band observed in each complex between 650 – 750 nm can be assigned to the Laporte forbidden ligand field transitions. In a square planar environment Cu(II), a d^9 metal ion, has $A_{1g} \leftarrow B_{1g}$, $B_{2g} \leftarrow B_{1g}$ and $E_g \leftarrow B_{1g}$ transitions, which have similar energy and hence remain merged to form a broad band. The transitions are usually seen as a broad band near 600 nm in normal copper complexes (**Table 4.2**). The lower energy of these transitions in complexes is indicative of significant distortion from planarity to weaken the ligand field.

Table 4.3 Electronic absorptions in the complexes of bis(picolinamide) ligands.

Complexes	**Charge transfer band in methanolic soln. (λ in nm)**	**d-d transition in methanolic soln. (λ in nm)**
$[Cu_2(picbu)_2](SO_4)_2.8H_2O$	215, 264, 306	702
$[Cu_2(pichx)_2](SO_4)_2.4H_2O$	214, 266, 308	688
$[Cu_2(phen)_2(picbu)](ClO_4)_4$	226, 271, 294	674
$[Cu_2(phen)_2(pichx)](ClO_4)_3(Ac)_1$	214, 300, 310	684
$[Cu_2(bipy)_2(picbu)](ClO_4)_4$	215, 271, 325	714
$[Cu_2(bipy)_2(pichx)(Ac)](ClO_4)_3$	260, 300, 310,	684
$[Cu_2(salac)_2(picbu)]$	232, 294, 325	654
$[Cu_2(salac)_2(pichx)].2H_2O$	220, 271, 300, 315	684
$[Cu_2(Brsalac)_2(picbu)]$	236, 268, 306	685
$[Cu_2(Brsalac)_2(pichx)]$	238, 268, 306	688

4.3.2 Infrared spectra:

The presence or absence of certain bands in the IR spectra have been, generally, utilized to illustrate the structure of the complexes. More important bands in the complexes are listed in, **Table 4.3.**

Absorption due to stretching of the amide N-H is observed between 3219 - 3371 cm^{-1} in the free ligand and complexes. The absorption due to the stretching of amide >C=O is observed between 1631-1647 cm^{-1} in the binuclear complexes, **4-I** to **4-X**. These are at lower energy compared to the free ligand value of 1657 cm^{-1}. The shift in the amide $\nu_{(>C=O)}$ towards lower energy in the complexes, indicates that the amide oxygen is involved in coordination with the Cu (II) ion. Also, the almost unaffected amide >N-H stretching frequency indicates that the amide nitrogen is not coordinated with the metal ion. Complexes, **4-I** and **4-II** show strong absorption bands at 1121 cm^{-1}, confirming the presence and the unidentate nature of sulphate ions [21]. In the IR spectra of the complexes, **4-III, 4-IV 4-V** and **4-VI,** ν_{as} of perchlorate is observed between 1090 – 1092 cm^{-1}. There is no splitting of the ~1090 cm^{-1} band indicating that perchlorate is tetrahedral and ionic i.e. not coordinated with the metal ions [21]. Complex **4-IV** has a strong band at 1428 cm^{-1} confirming the presence of acetate. The value corresponding to the stretching in acetate also confirms that the acetate ion is not coordinated and is present out side the coordination sphere [21]. In complex **4-VI** a band appears at 1315 cm^{-1} corresponding to ν_s in acetate. The energy of this vibration confirms the unidentate mode of coordination of acetate ion with the metal ion. The presence of water molecules in the complexes **4-I, 4-II, 4 -VIII, 4-XI** and **4-XII** results in the appearance of a broad band in the 3450 – 3650 cm^{-1} region due to the vibrations of OH in lattice water.

Other bands characteristic of ligands include asymmetric stretching between 2923 – 2945 cm^{-1} and symmetric stretching between 2840 – 2875 cm^{-1} due to the presence of $-CH_2$ groups, –C=C- stretching in aromatic ring is observed between 3066 – 3090 cm^{-1} and stretching of the >C=N (ring) appears between 1598 – 1606 cm^{-1} (**Fig. 4.5.1** to **Fig. 4.6.6**). Thus, the IR spectra support the suggested structures of the complexes.

Table 4.3 IR absorptions (cm^{-1}) of the ternary binuclear complexes.

Comp. No.	ν(-NH) stretching	aromatic stretching ν(-C-H)	$\nu_{as}(-CH_2)$ and $\nu_s(-CH_2)$	ν(>C=O) (cm^{-1})	ring stretching ν(-C=N)	miscellaneous frequencies
4-I	3234	3090	2940, 2855	1633	1604	$\nu(SO_4)$1121
4-II	3219	3066	2930, 2862	1636	1603	$\nu(SO_4)$1121
4-III	3341	3071	2923, 2856	1636	1606	$\nu(ClO_4)$1090
4-IV	3341	3071	2932, 2857	1643	1598	$\nu(ClO_4)$1090, $\nu(CH_3COO)$1428
4-V	3367	3086	2940, 2840	1637	1604	$\nu(ClO_4)$1091
4-VI	3361	3083	2933, 2863	1647	1601	$\nu(ClO_4)$1092, $\nu(CH_3COO)$1315
4-VII	3228	3066	2926, 2865	1633	1600	-
4-VIII	3368	3067	2931, 2862	1638	1601	-
4-IX	3223	3068	2929, 2865	1638	1591	ν(C-Br)1100
4-X	3233	3071	2927, 2870	1631	1592	ν(C-Br)1097

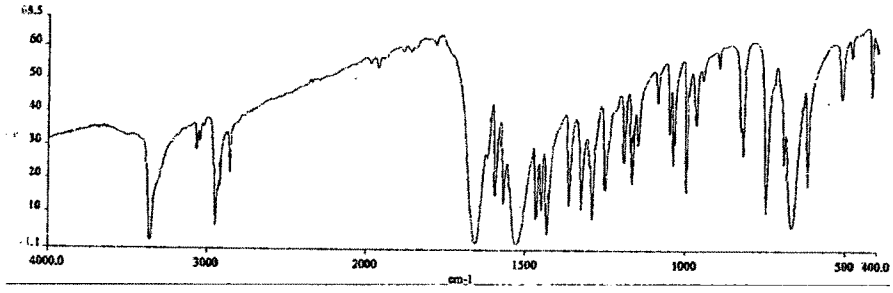

Fig. 4.5.1 FTIR spectrum of the ligand, picbu.

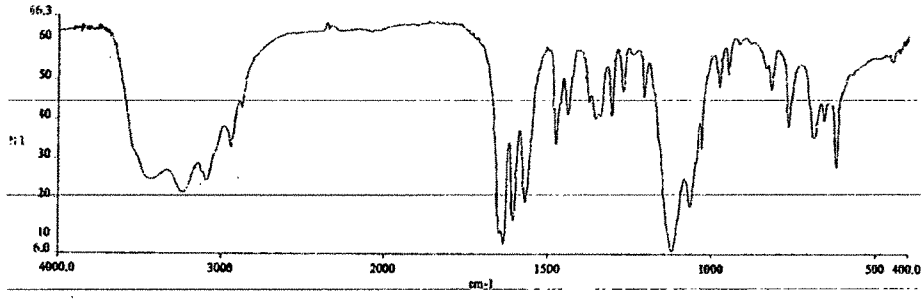

Fig. 4.5.2 FTIR spectrum of the binuclear complex, $[Cu_2(picbu)_2](SO_4)_2].8H_2O$.

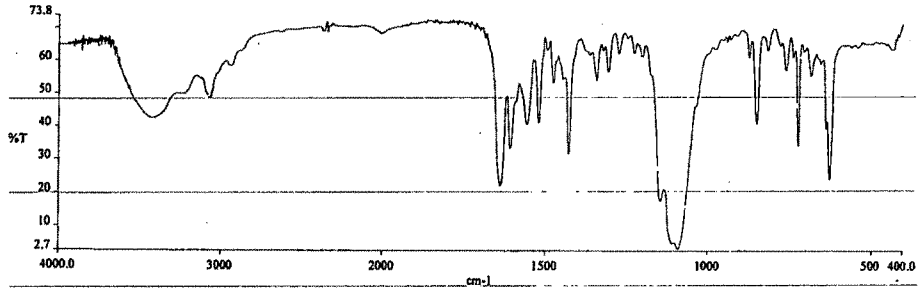

Fig. 4.5.3 FTIR spectrum of the binuclear complex, $[Cu_2(phen)_2(picbu)](ClO_4)_4$.

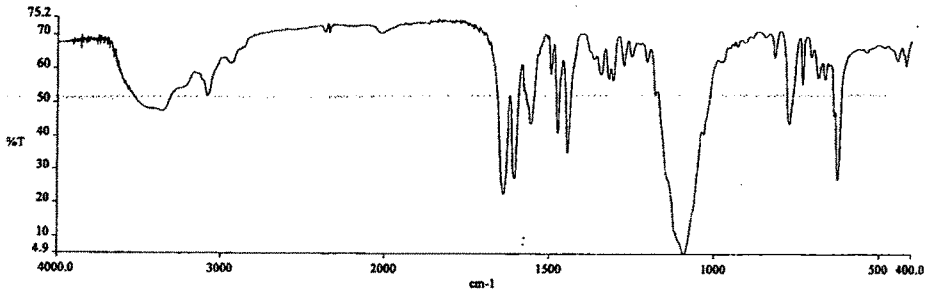

Fig. 4.5.4 FTIR spectrum of the binuclear complex, $[Cu_2(bipy)_2(picbu)](ClO_4)_4$.

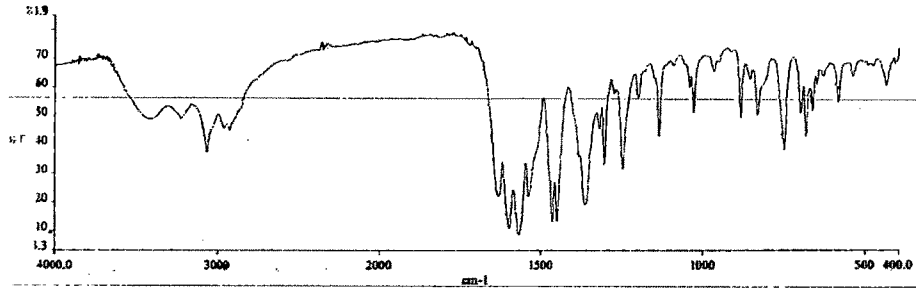

Fig. 4.5.5 FTIR spectrum of the binuclear complex, $[Cu_2(salac)_2(picbu)]$.

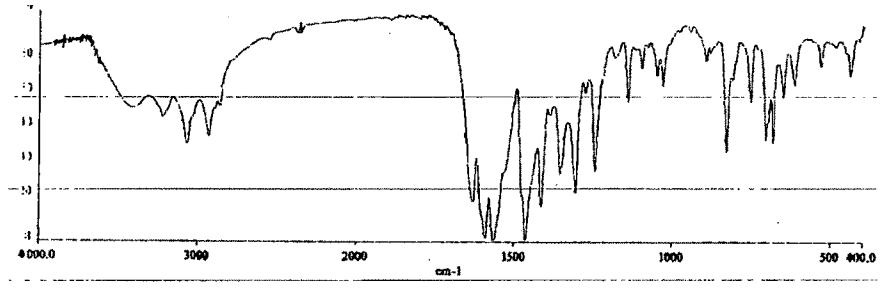

Fig. 4.5.6 FTIR spectrum of the binuclear complex, $[Cu_2(Brsalac)_2(picbu)]$.

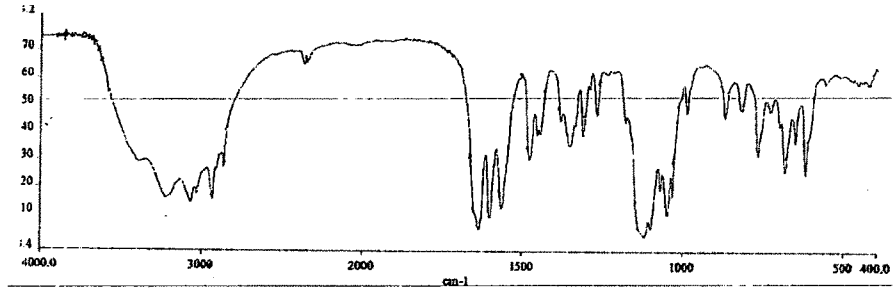

Fig. 4.6.1 FTIR spectrum of the ligand, pichx.

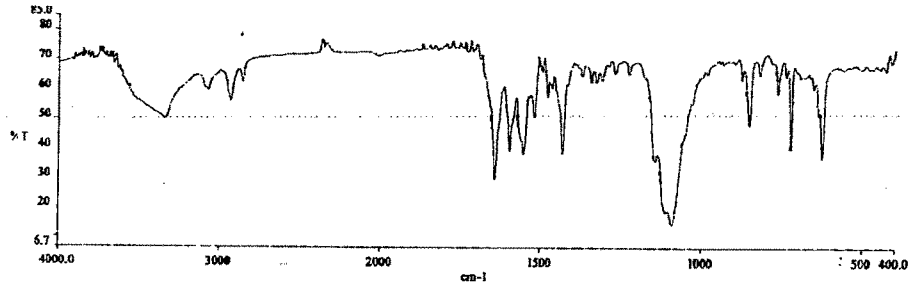

Fig. 4.6.2 FTIR of the binuclear complex, $[Cu_2(pichx)_2](SO_4)_2].4H_2O$

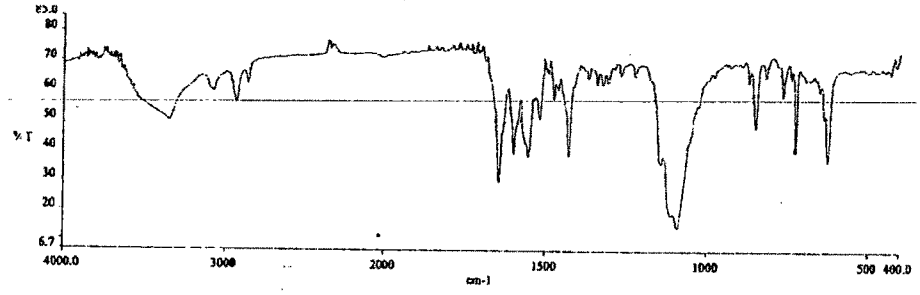

Fig. 4.6.3 FTIR spectrum of the binuclear complex, $[Cu_2(phen)_2(pichx)](ClO_4)_3(Ac)_1$.

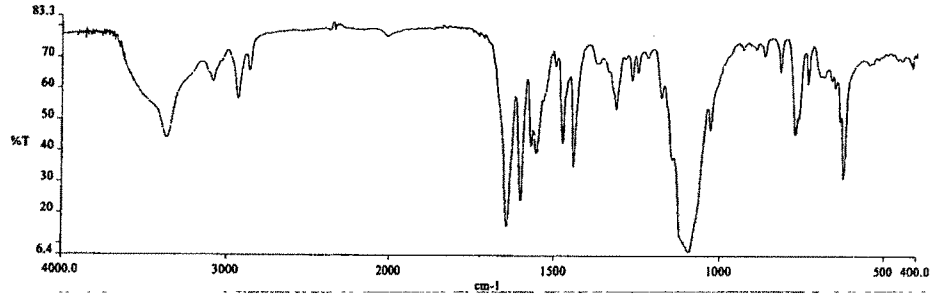

Fig. 4.6.4 FTIR spectrum of the binuclear complex, $[Cu_2(bipy)_2(pichx)(Ac)](ClO_4)_3$.

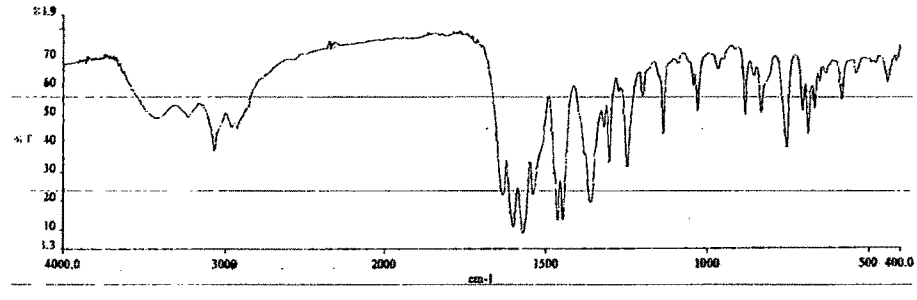

Fig. 4.6.5 FTIR spectrum of the binuclear complex, $[Cu_2(salac)_2(pichx)].2H_2O$.

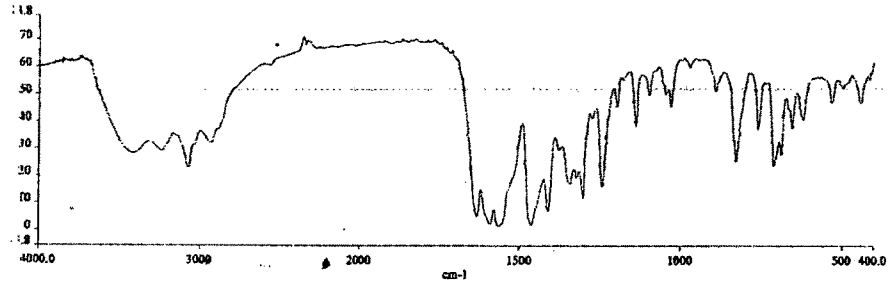

Fig. 4.6.6 FTIR spectrum of the binuclear complex, $[Cu_2(Brsalac)_2(pichx)]$.

4.4.3 Mass Spectra:

The FAB mass spectrum of the complex, $[Cu_2(salac)_2(picbu)]$ was recorded (**Fig. 4.7**). The parent ion peak can be observed at m/z = 697. This is formed by protonation of the complex molecule, $[M+H^+]$.

A peak corresponding to binucleating ligand, $[picbu+H]^+$ appears at m/z = 299 with 14% relative abundance. This fragment undergoes further fragmentation to give other related species at m/z = 141 (7%) and m/z = 89 (26%).

The peaks observed at m/z = 380, 362, 350 and 307 with relative abundance 5%, 11%, 5% and 19%, respectively, strongly elucidate the formation of binuclear complexes with general formula $[Cu_2 (AA)_2(picbu)]$.

Some important fragments with the observed m/z values are summarized in **Table 4.4** and the fragments formed are represented below.

The peak corresponding to the fragments of m-nitrobenzyl alcohol and associated products are observed at m/z 136, 137, 154, 289 and 307 with high relative aboundance. These fragments can get associated with various fragments of the binuclear complex and thus are responsible for the occurrence of widely distributed peak with low relative abundance.

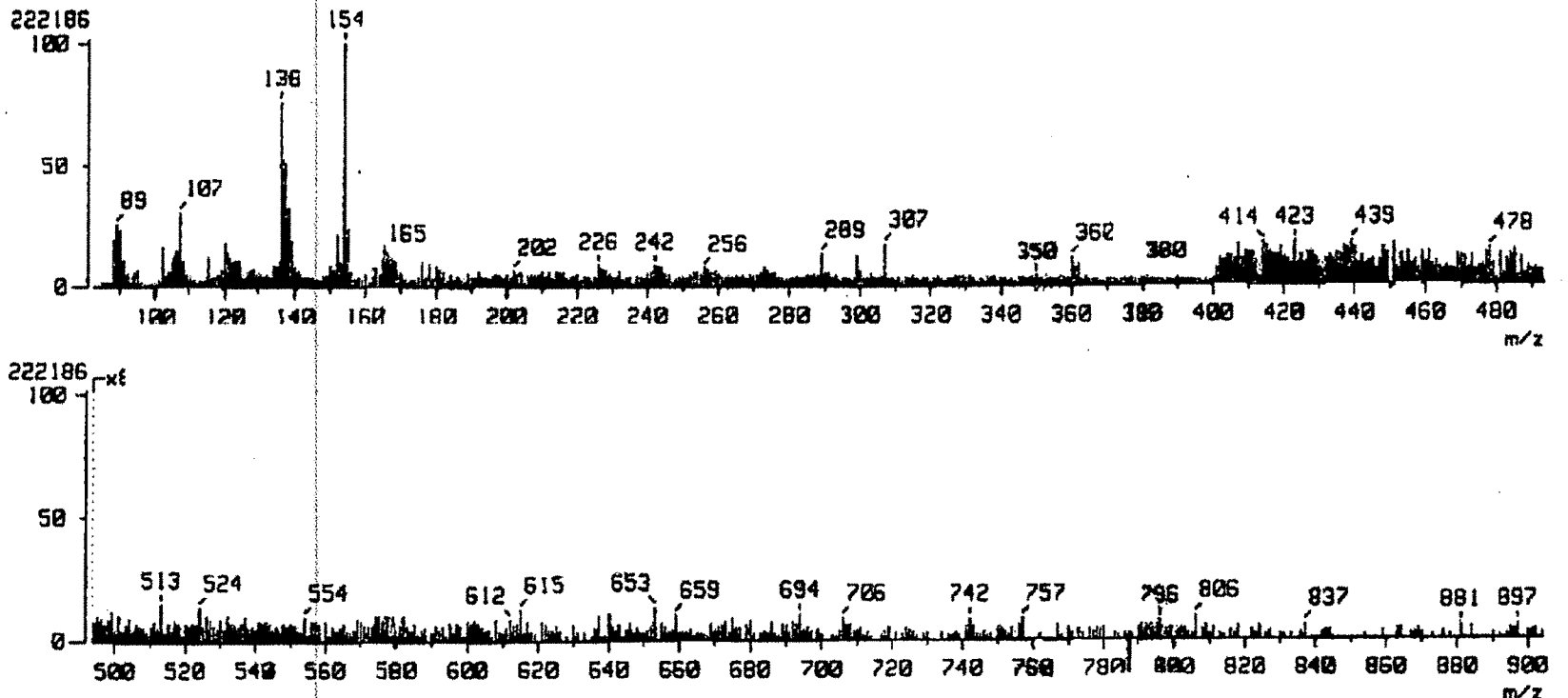

Fig 4.7 FAB-Mass spectra of binuclear complex, $[Cu_2(salac)_2(picbu)]$

Table 4.4 Fragmentation pattern in the positive ion FAB-MS of $[Cu_2(salac)_2(picbu)]$ in m-nitrobenzyl alcohol.

m/z (% relative abundance)	**Molecular formula of the fragments**
697 (8%)	$[C_{30}H_{27}O_8N_4Cu_2]^+$ (parent ion, $[M+H]^+$)
560 (10%)	$[C_{23}H_{22}O_5N_4Cu_2]^+$
423 (20%)	$[C_{16}H_{17}O_2N_4Cu_2]^+$
360 (15%)	$[C_{16}H_{17}O_2N_4Cu]^+$
299 (14%)	$[C_{16}H_{19}O_2N_4]^+$ (binucleating ligand)
380 (5%)	$[C_{17}H_{21}O_4N_2Cu]^+$
362 (11%)	$[C_{16}H_{15}O_4N_2Cu]^+$
350 (5%)	$[C_{15}H_{15}O_4N_2Cu]^+$
307 (19%)	$[C_{13}H_{10}O_4NCu]^+$
202 (8%)	$[C_7H_7O_3Cu]^+$ [Cu salcylate]$^+$
141 (7%)	$[C_6H_9O_2N_2]^+$
138 (34%)	$[C_7H_6O_3]^+$ (salicylic acid)
89 (26%)	$[NH_2\text{-}(CH_2)_4\text{-}NH_3]^+$ (amine)
757 (9 %)	$[C_{30}H_{24}O_8N_4Cu_3]^+$, (M+Cu)

Possible structure of the complex, $[Cu_2(salac)_2(picbu)_2]$ and the corresponding fragments in FAB-Mass spectrum:

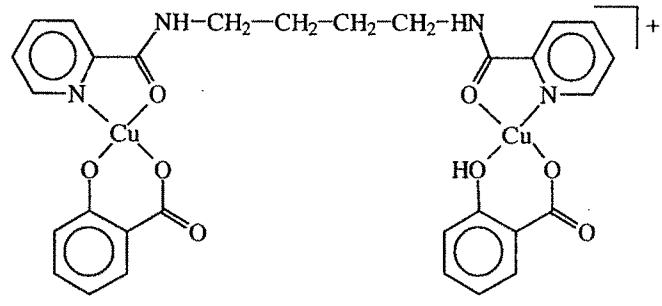

m/z 697 (8%), $[C_{30}H_{27}O_8N_4Cu_2]^+$

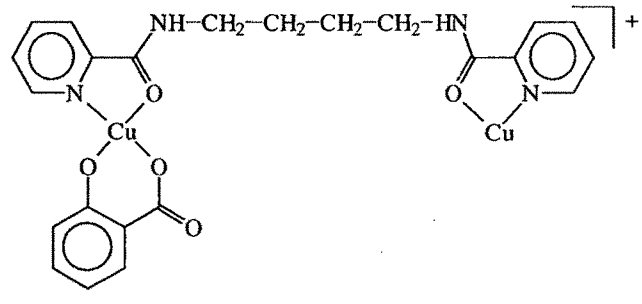

m/z 560 (10%), $[C_{23}H_{22}O_5N_4Cu_2]^+$

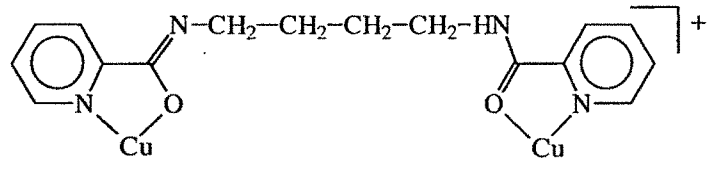

m/z 423 (20%), $[C_{16}H_{17}O_2N_4Cu_2]^+$

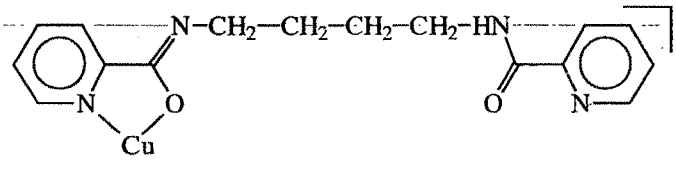

m/z 360 (15%), $[C_{16}H_{17}O_2N_4Cu]^+$

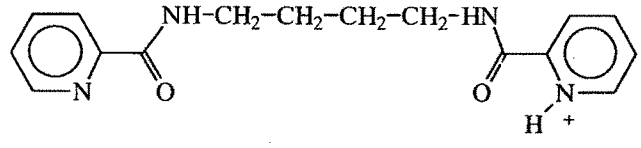

m/z 299 (14%), $[C_{16}H_{19}O_2N_4]^+$

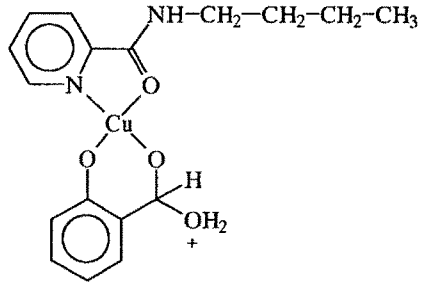

m/z 380 (5%), $[C_{17}H_{21}O_4N_2Cu]^+$

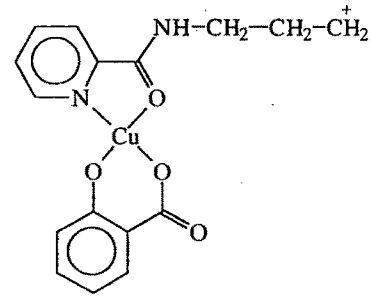

m/z 362 (11%), $[C_{16}H_{15}O_4N_2Cu]^+$

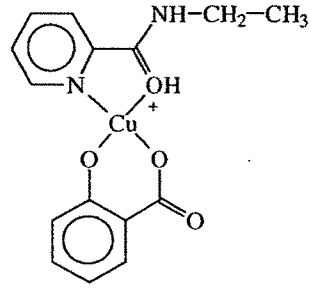

m/z 350 (5%), $[C_{15}H_{15}O_4N_2Cu]^+$

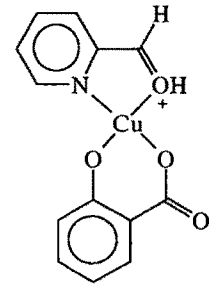

m/z 307 (19%), $[C_{13}H_{10}O_4NCu]^+$

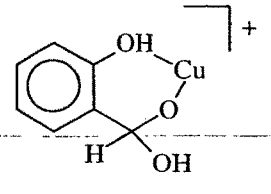

m/z 202 (8%), $[C_7H_7O_3Cu]^+$

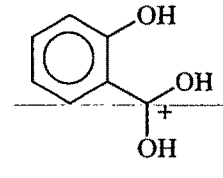

m/z 139 (8%), $[C_7H_7O_3]^+$

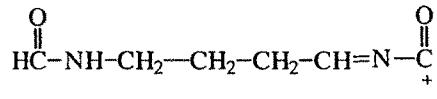

m/z 141 (7%), $[C_6H_9O_2N_2]^+$

$NH_2—CH_2—CH_2–CH_2–CH_2–\overset{+}{N}H_3$

m/z 89 (26%), $[C_4H_{13}N_2]^+$

4.3.4 ESR spectral studies:

The ESR spectrum of complex $[Cu_2(salac)_2(picbu)]$ was recorded at room temperature in the polycrystalline solid state and at LNT in the form of frozen solution in DMF (**Fig 4.8.1** & **Fig 4.8.2**). The g values are shown in **Table 4.5**. Both spectra are identical with g values supporting square planar geometry around the metal centre. A half field transition is observed at RT and at LNT in the frozen solution confirming the presence of intra molecular spin-spin interaction through the σ – orbitals in the bridging molecule.

Table 4.5 ESR of the $[Cu_2(salac)_2(picbu)]$

	Room temperature	**Liquid N_2 temperature**
$g_{\parallel}$	2.17023	2.16687
$g_{\perp}$	2.08783	2.08662

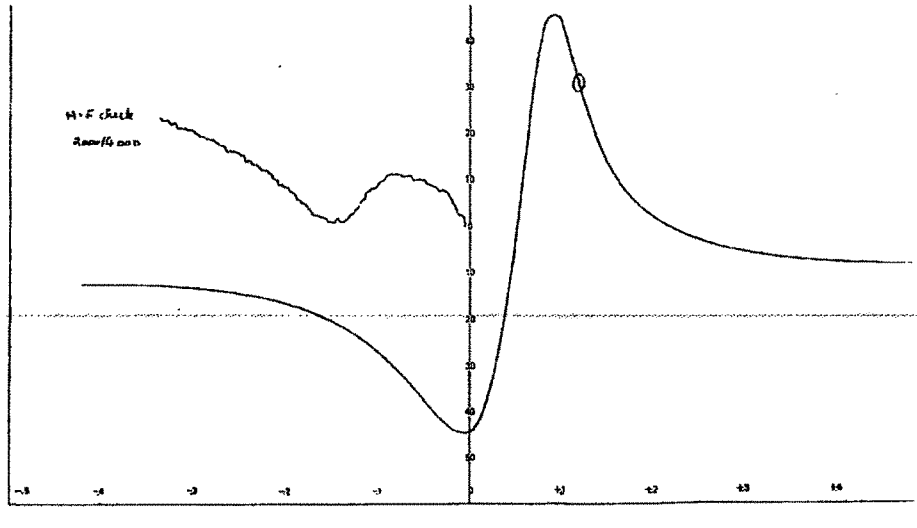

Fig.4.8.1 ESR of binuclear complex, $[Cu_2(salac)_2(picbu)]$ at RT.

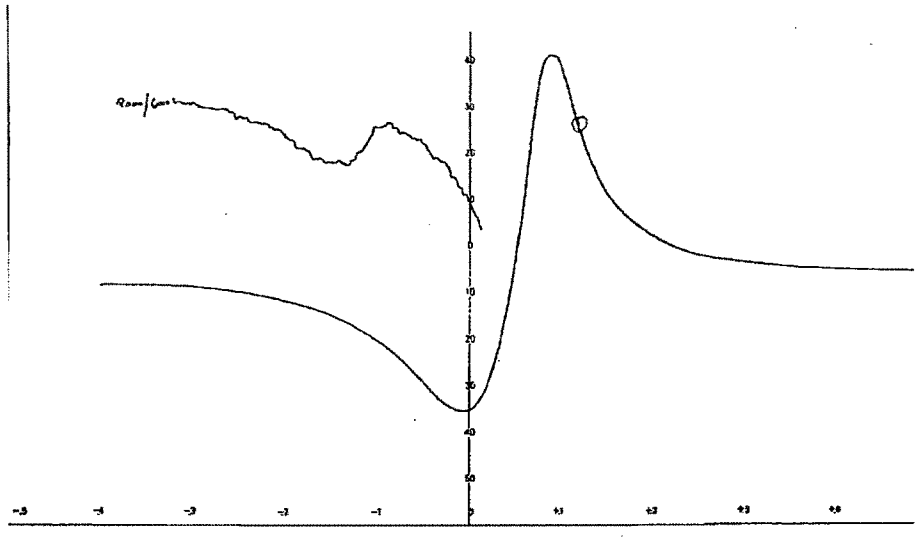

Fig.4.8.2 ESR of binuclear complex, $[Cu_2(salac)_2(picbu)]$ at LNT.

4.3.5 Magnetic Properties:

The magnetic susceptibility of complexes, **4-III, 4-V** and **4-VII** were measured from liq. N_2 to room temperature. The least squares fit of the data (**Fig. 4.10.1 to Fig. 4.10.3**) to Bleaney – Bower's equations yielded positive J values ranging between 9 to 73 cm^{-1}. This indicates a weak to moderately strong ferromagnetic exchange between the metal centers in these complexes through σ – bonded bridging groups.

Hendrickson and coworkers [15] first time suggested that the σ – orbitals can participate in the super exchange over a long distance in multiatomic bridges. The role of σ – orbitals in superexchange interaction has been further supported by the study of spin exchange interaction in the binuclear complexes, bearing the following saturated bridging moieties **Fig. 4.9**, [22].

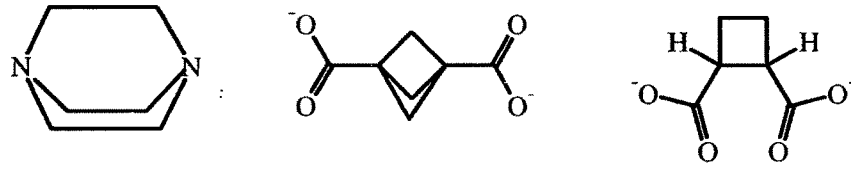

Fig. 4.9.

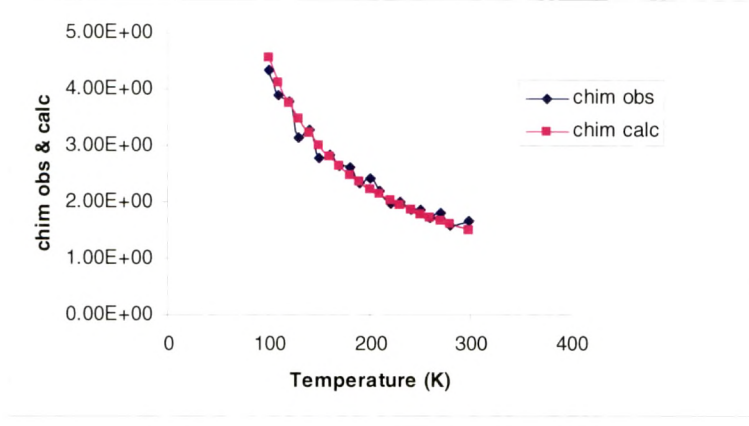

Fig. 4.10.1 $[Cu_2(bipy)_2(picbu)](ClO_4)_4$

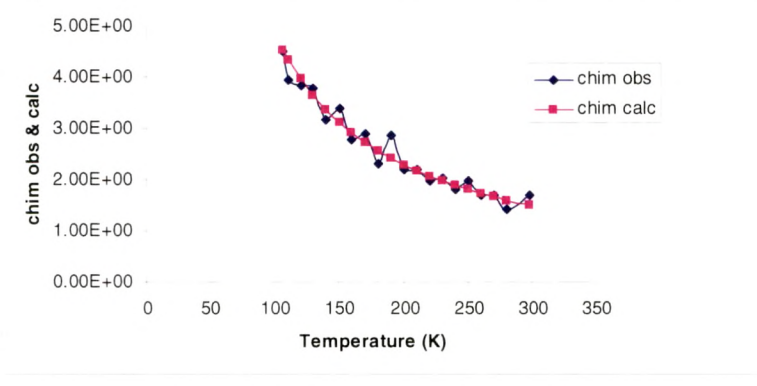

Fig. 4.10.2 $[Cu_2(phen)_2(picbu)](ClO_4)_4$

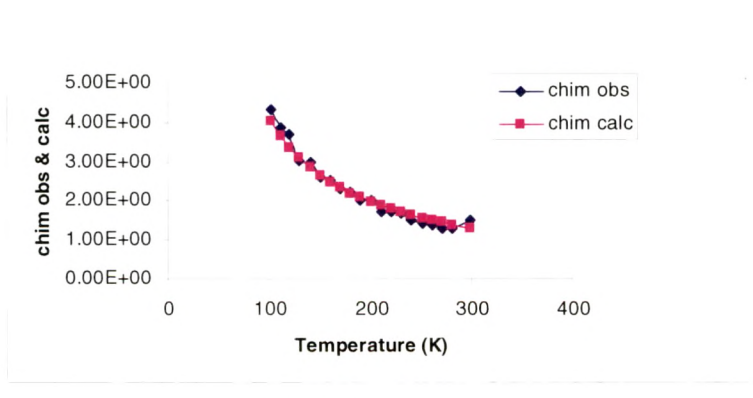

Fig. 4.10.3 $[Cu_2(salac)_2(picbu)]$

These binuclear complexes were reported to have antiferromagnetic interaction, between the two paramagnetic centers, yet the extent of interaction is low.

In these binuclear complexes, bearing aliphatic bridging moieties, the absence of the interdimer interaction has been confirmed from the structural data obtained from the single crystal X-ray diffraction studies [19]. The intermolecular distances are too far, for any inter dimer interaction. Thus, in these complexes, the antiferromagnetic interaction is intramolecular and is purely through the σ – bonding orbitals of the aliphatic bridging moieties.

It is appropriate to recall at this stage that in multi atomic bridging ligands some molecular orbital with appropriate energy and symmetry is usually available to mediate the exchange. This ligand mediated interaction between paramagnetic orbitals over the metal ion should result in the formation of new metal centered MO's as shown in Ch. 2 (**Fig. 2.17**). It can be expected that the orientation of paramagnetic metal orbitals with respect to each other must be an important factor deciding the effective overlap between these orbitals and hence the extent of magnetic exchange.

In order to examine this, systematic variations have been made in the non bridging ligand in the complexes. The geometry of the complexes was optimized using universal force field [23, 24]. The torsional angle between the metal coordination planes has been calculated. In a series of complexes with same binucleating diamide ligand and bipy, salac or phen as the non bridging secondary ligand, the torsional angle varies from 100° to 121° (**Table4.6**).

Table 4.6 J, g and Torsional angle of some complexes.

Complexes	**J (cm^{-1})**	**Torsional angle**	**g**
$[Cu_2(bipy)_2(picbu)](ClO_4)_4$	9.9	108.96	2.12
$[Cu_2(salac)_2(picbu)]$	23.1	119.56	1.95
$[Cu_2(phen)_2(picbu)](ClO_4)_4$	73.0	120.98	1.99

The values in **Table 4.6** indicate that the J values increase with increase in deviation in torsional angle from 180°. As the torsional angle deviates more from 180°, the metal coordination is no longer coplanar. This results in the mismatch of the overlapping metal ion orbitals with molecular orbitals of the bridging ligand and leads to ferromagnetic interaction. The variation in geometry and in the J values is a result of change in the nature of non-bridging ligand. D. Zhang et al [25] have observed similar dependence of the extent of magnetic exchange on the non bridging ligands in the complexes with oxalodiamide bridging groups.

In the present complexes the bis(picolylamide) bridging ligand is common while the non bridging secondary ligand changes from bipy to salac to phen. Results shows that to the first approximation bulkier and more π-bonding ligands can distort the metal coordination planes to a greater extent and hence lead to stronger ferromagnetism.

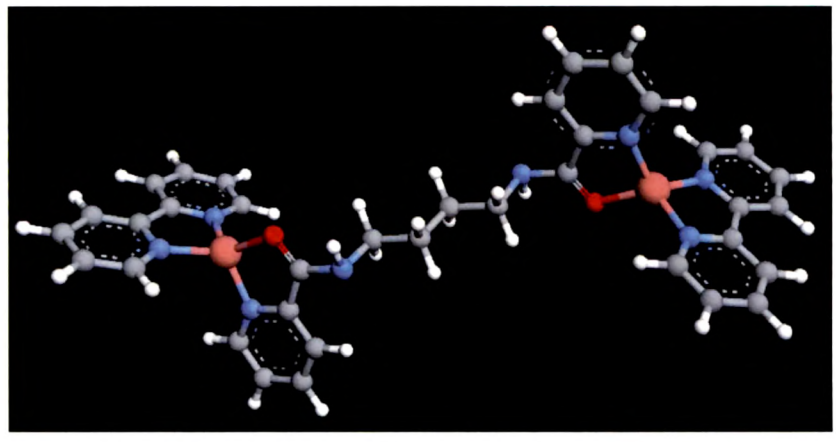

Fig. 4.11.1 Optimized geometry of the binuclear complex, $[Cu_2(bipy)_2(picbu)](ClO_4)_4$

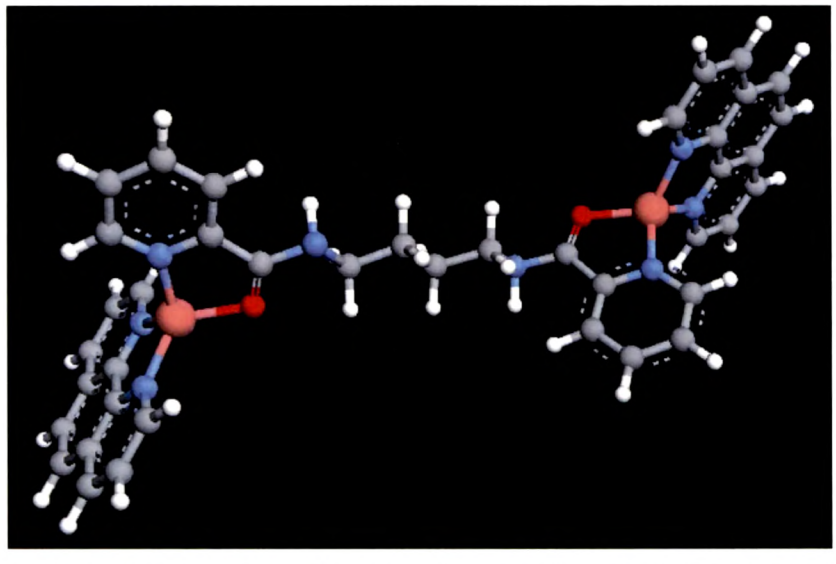

Fig. 4.11.2 Optimized geometry of the binuclear complex, $[Cu_2(phen)_2(picbu)](ClO_4)_4$

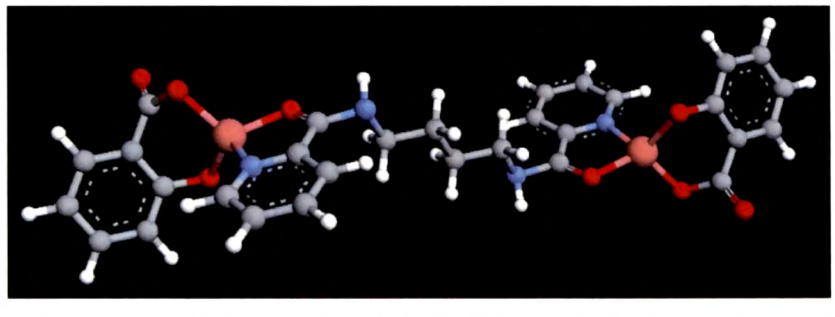

Fig. 4.11.3 Optimized geometry of the binuclear complex, $[Cu_2(salac)_2(picbu)]$.

4.4 References:

[1] J. D. Crane, D. E. Fenton, J. M. Latour, A. J. Smith, *J. Chem. Soc. Dalton Trans, 1991, 2979.*

[2] Copper Proteins, Copper Enzymes, R. Lontie (Eds), *CRC Press: Boca Raton, FL, Vol. I-III (1984).*

[3] H. J. Beinert, *Inorg. Biochem., 1991,* ***44,*** *173.*

[4] E.I. Soloman, M. D. Lowery, D. E. Root, B. L. Hemming, *Mechanistic Bioinorganic Chemistry, American Chemical Society, Washington, DC, (1995).*

[5] J. J. R. Fausto da Silva, R. J. P. Williams, *The Biological Chemistry of the Elements, Oxford University Press: Oxford, U. K. (1991).*

[6] E. I. Solomon, D. E. Wilcox in R. D. Willett, D. Gatteschi, O. Kahn (Eds), *Magneto – Structural Correlations in Exchange Coupled Systems, D. Reidel, Dordrech (1985) 463.*

[7] D. N. Hendrickson, in Magneto – Structural Correlations in Exchange Coupled Systems (Eds) R. D. Willett, D. Gatteschi, O. Kahn, NATO ASI Ser. No. 140, Reidel Dordrecht, (1985) 523.

[8] O. Kahn, *Adv. Inorg. Chem., 1996,* ***43****, 179.*

[9] O. Kahn, *Structure Bonding (Berlin), 1987,* ***68,*** *89.*

[10] W. E. Hatfield, *Comments Inorg. Chem, 1981,* ***1****, 105.*

[11] D. J. Hodgson, *Prog. Inorg. Chem., 1975,* ***21****, 209.*

[12] Van H. Crawford, H. W. Richardson, J. R. Wasson, D. J. Hodgson, W. E. Hatfield, *Inorg. Chem., 1976,* ***15****, 2107.*

[13] M. Melnik, *Coord. Chem. Rev.,1982,* ***42****, 259.*

[14] M. Kato, Y. Muto, *Coord. Chem. Rev., 1988,* ***92****, 45.*

[15] T. R. Felthouse, D. N. Hendrickson, *Inorg. Chem., 1978,* ***17****, 2636.*

[16] P. Chaudhury, K. Order, K. Wieghardt, S. Ghering, W. Hasse, B. Nuber, J. Weiss, *J. Am. Chem. Soc., 1988,* ***110****, 3657.*

[17] J. Glerup, P. A. Goodson, D. J. Hodgson, K. Michelsen, *Inorg. Chem., 1995,* ***34****, 6255.*

[18] J. A. Real, M. Mollar, R. Ruiz, J. Faus, F. Lloret, M. Julve, M. P. Levsalles, *J. Chem. Soc. Dalton Trans, 1993, 1483.*

[19] R. Calvo, C. A. Steren, O. E. Piro, T. Rojo, F. J. Zungia, E. E. Castellano, *Inorg. Chem., 1993, **32**, 6016.*

[20] *Beil., **10**, 107.*

[21] K. Nakamoto, Infrared and Raman Spectra of Inorganic and Coordination Compounds : Part B, 5th Eds, *Wiley – Interscience New York, 1997.*

[22] A. W. Clauss, S. R. Wilson, R. M. Buchanan, C. G. Pierpont, D. N. Hendrickson, *Inorg. Chem, 1983, 22, 628.*

[23] Journal Citations for this Calculation:-

[23.a] M. A. Thompson, M. C. Zerner, *J. Am. Soc., 1991, **113**, 8210.*

[23.b] M. A. Thompson, E. D. Glendening, D. Feller, *J. Phys. Chem., 1994, **98**, 10465.*

[23.c] M. A. Thompson, G. K. Schenter, *J. Phys. Chem., 1995, **99**, 6374.*

[23.d] M. A. Thompson, *J. Phys. Chem., 1996, **100**, 14492.*

[24] UFF references:-

[24.a] A. K. Rappe, et. al., *JACS, 1992, **114**, 10024.*

[24.b] C. J. Casewit, K. S. Colwell, A. K. Rappe, *JACS, 1992, **114**, 10035.*

[24.c] C. J. Casewit, K. S. Colwell, A. K. Rappe, *JACS, 1992, **114**, 10046.*

[24.d] A. K. Rappe, W. A. Goddard, *JPC, 1991, **95**, 3358.*

[24.e] A. K. Rappe, K. S. Colwell, C. J. Casewit, *Inorg. Chem., 1993, 32, 3438.*

[25] Z. Liu, Z. Lu, D. Zhang, Z. Jiang, L. Li, C. Liu, D. Zhu, *Inorg. Chem. 2004, 43, 6620.*